The Journal of Chemical Physics

Prediction of Kapitza resistance at fluid-solid interfaces

Cite as: J. Chem. Phys. **151**, 194502 (2019); https://doi.org/10.1063/1.5126887
Submitted: 06 September 2019 . Accepted: 29 October 2019 . Published Online: 18 November 2019

Sobin Alosious, Sridhar Kumar Kannam, Sarith P. Sathian, and B. D. Todd

View Online Export Citation CrossMark

ARTICLES YOU MAY BE INTERESTED IN

Flow of water through carbon nanotubes predicted by different atomistic water models
The Journal of Chemical Physics **150**, 194501 (2019); https://doi.org/10.1063/1.5086054

The role of water models on the prediction of slip length of water in graphene nanochannels
The Journal of Chemical Physics **151**, 174705 (2019); https://doi.org/10.1063/1.5123713

Macroscopic relations for microscopic properties at the interface between solid substrates and dense fluids
The Journal of Chemical Physics **150**, 214705 (2019); https://doi.org/10.1063/1.5094911

Lock-in Amplifiers
... and more, from DC to 600 MHz
Watch

© 2019 Author(s).

The Journal of Chemical Physics ARTICLE scitation.org/journal/jcp

Prediction of Kapitza resistance at fluid-solid interfaces

Cite as: J. Chem. Phys. 151, 194502 (2019); doi: 10.1063/1.5126887
Submitted: 6 September 2019 • Accepted: 29 October 2019 •
Published Online: 18 November 2019

View Online Export Citation CrossMark

Sobin Alosious,[1,2] Sridhar Kumar Kannam,[2] Sarith P. Sathian,[1] and B. D. Todd[2,a)]

AFFILIATIONS

[1] Department of Applied Mechanics, Indian Institute of Technology Madras, Chennai 600036, India
[2] Department of Mathematics, Faculty of Science, Engineering and Technology, Swinburne University of Technology, Melbourne, Victoria 3122, Australia

[a)] Electronic mail: btodd@swin.edu.au

ABSTRACT

Understanding the interfacial heat transfer and thermal resistance at an interface between two dissimilar materials is of great importance in the development of nanoscale systems. This paper introduces a new and reliable linear response method for calculating the interfacial thermal resistance or Kapitza resistance in fluid-solid interfaces with the use of equilibrium molecular dynamics (EMD) simulations. The theoretical predictions are validated against classical molecular dynamics (MD) simulations. MD simulations are carried out in a Lennard-Jones (L-J) system with fluid confined between two solid slabs. Different types of interfaces are tested by varying the fluid-solid interactions (wetting coefficient) at the interface. It is observed that the Kapitza length decreases monotonically with an increasing wetting coefficient as expected. The theory is further validated by simulating under different conditions such as channel width, density, and temperature. Our method allows us to directly determine the Kapitza length from EMD simulations by considering the temperature fluctuation and heat flux fluctuations at the interface. The predicted Kapitza length shows an excellent agreement with the results obtained from both EMD and non-equilibrium MD simulations.

Published under license by AIP Publishing. https://doi.org/10.1063/1.5126887

I. INTRODUCTION

Recent advancements in nanoscience and technology have resulted in a large number of investigations into the transport of mass, momentum, and energy in nanoconfinement systems.[1,2] A clear understanding of interfacial heat transfer and thermal resistance at fluid-solid interfaces is crucial in the designing of various micro/nanoscale electronic, photonic, and phononic devices.[3] When there is a heat transfer across an interface between two dissimilar materials, a temperature discontinuity occurs due to the thermal resistance at that interface. This thermal resistance, due to the difference in the electronic and vibrational properties of the two materials in contact, is called the interfacial thermal resistance and is given by

$$R_k = \frac{\Delta T}{J_q}, \tag{1}$$

where ΔT is the temperature difference between the materials in contact and J_q is the interface heat flux. The interfacial thermal resistance across the fluid-solid interface is also known as the Kapitza resistance. In 1941, Kapitza discovered a strong thermal resistance across a solid interface which was in contact with superfluid helium (<2 K).[4] Later, Khalatnikov illustrated a theoretical model in which the interfacial thermal resistance is recognized as a general phenomenon associated with all interfaces in all temperature ranges.[5] However, the measured heat flux across the solid-superfluid interface is approximately two orders of magnitude higher than the prediction of Khalatnikov. Also, confined fluids at the nanoscale (within a few molecular diameters) may break classical theories such as Navier-Stokes equations and the no-slip boundary condition.[6,7]

The experimental study of interfacial heat transfer in nanoscale systems is complex due to the difficulty of fabricating and handling these objects at length scales below ≈10 nm. These challenges can be overcome by using computational tools, such as classical molecular dynamics (MD) simulation techniques, which allows the modeling of molecular structure and its interactions at atomic length and time scales precisely. Calculation of transport coefficients using

Published under license by AIP Publishing

either equilibrium or nonequilibrium molecular dynamics (NEMD) simulation methods has proven effective in many scenarios. The well known Green-Kubo formulas[8] can be used for calculating transport coefficients using equilibrium molecular dynamics (EMD) simulations. An alternate way to compute the transport coefficients is the nonequilibrium molecular dynamics simulation method, in which the corresponding gradients and fluxes are measured directly, similar to an experimental method.[9,10] Both methods are mainly focused on bulk transport coefficients such as viscosity, diffusion coefficient, and thermal conductivity. However, the transport process at the interface has received less attention. Of these, the Kapitza resistance is one of the important interfacial properties in heat transfer problems. A more convenient term used instead of the Kapitza resistance is called the Kapitza length and is defined by

$$L_k = R_k \kappa, \tag{2}$$

where κ is the thermal conductivity of either the solid or fluid phase. L_k is similar to the slip length in fluid flow and can be defined as the additional thickness of material required to achieve the same heat transfer in place of the thermal resistance at the interface. This additional thickness can be measured either in the direction of solid or fluid from the interface as per convenience. The thermal conductivity of the solid phase is used in Eq. (2) to determine the Kapitza length toward the fluid side and vice versa.

Researchers have developed different techniques to calculate the interfacial thermal resistance. Also, different types of interfaces such as solid-solid, fluid-solid, gas-solid, and fluid-gas are treated separately. Liang and Hu[11] reviewed different methods used for understanding interfacial transport behavior for different types of interfaces such as solid-solid, solid-liquid, and solid-gas interfaces using MD simulations. They have also compared the pros and cons of other MD techniques such as first-principles MD and approach-to-equilibrium MD. One of the most popular methods for calculating the Kapitza resistance is the NEMD method. The NEMD simulation comprises of an initial equilibration of the system to the required reference temperature and pressure, followed by the addition of a heat source and a heat sink on both end layers of the system, respectively, which will create a temperature gradient across the system. The interfacial thermal resistance can be directly determined by Eq. (1) once the system reaches the steady state. Numerous studies using the NEMD method have been carried out to understand the interfacial heat transfer mechanism which allows us to reduce the Kapitza resistance and enhance the heat transfer across interfaces by varying the temperature, pressure, and chemical functionalization at the interface.[12–15] In NEMD simulations, the external driving forces such as heat flux required to provide an input are several orders of magnitude higher than the actual driving forces in experiments, which is due to the small system size and simulation time compared to experiments.[16] Therefore, the response of the system should be maintained at the linear response regime, such that the simulation data can be extrapolated down to experimental conditions. Performing NEMD simulations at several external forces allows us to identify the linear regime. Another challenge in the calculation of the Kapitza resistance using NEMD simulation is the finite size effect. Several studies reported that if the thickness of the materials composing the interface is comparable with the bulk phonon mean free path, then the results of the Kapitza resistance is size-dependent.[17–20] Liang and Keblinski[21] studied the role of finite size effects on the calculation of the Kapitza resistance between solid-solid interfaces described by high phonon mean free paths. They have also used an EMD method to extract a size-independent interfacial thermal resistance from the time integral of the heat flux autocorrelation function. The heat transfer between solids and fluids in which nanoparticles are embedded is also an area of research interest as is the case of the effect of the interface curvature on the Kapitza resistance.[22–24] In addition, Muscatello *et al.*[25] recently studied the heat transfer between fluid-vapor interfaces and demonstrated through NEMD simulation how structural features at the interface determine the transport mechanisms. Several NEMD studies have been carried out to investigate the Kapitza resistance between various types of interfaces, and different methods to control it have been suggested, which may be useful in a number of practical scenarios. Hu and Sun[26] studied the influence of surface nanopatterns on the Kapitza resistance between a gold surface and boiling water. They found that the Kapitza resistance is not affected by the phase change of water. However, a reduction in the Kapitza resistance can be achieved by increasing the height of nanopatterns due to the rise in interaction energy per unit area. Also, it is possible to reduce the Kapitza resistance by increasing the width-to-spacing ratio of the nanopatterns. Pham *et al.*[27] investigated the impacts of bulk liquid pressures on the Kapitza length at water/solid interfaces and observed different behaviors of liquid water in the vicinity of gold and silicon surfaces. They found that the distance between the gold surface and the first density peak layer of water was constant and was not affected by the change in bulk liquid pressure. However, the same parameter directly depends on the bulk liquid density for the silicon surface. These findings show that the effect of pressure on the Kapitza resistance cannot be generalized and it depends on the wettability of the surface in contact. Ramos-Alvarado *et al.*[28] characterized the interfacial thermal resistance between a silicon surface and water in terms of wetting properties of the surfaces. They found that the interfacial heat transfer is not primarily correlated with the wettability, which is characterized by the work of adhesion and contact angle. Instead, they suggested that the fundamental parameter for explaining interfacial thermal transport is the density depletion length, similar to the hydrodynamics of liquids in nanoconfinement. Han *et al.*[29] studied the interfacial heat transfer between a gold surface and a suspension of ethanol containing gold nanoparticles. They found that the Kapitza resistance increases with the addition of nanoparticles due to the weakening of fluid-solid interaction strength. This increase in the Kapitza resistance causes a shift in the boiling temperature at the nanofluid/solid interface compared to pure ethanol. They found this effect to be significant even for a small concentration of nanoparticles.

The calculation of the Kapitza resistance from an EMD method gives several advantages over NEMD methods. Unlike NEMD, there is no need to identify the linear regime for the EMD method, which allows the calculation of the Kapitza resistance from a single simulation. Different studies have been carried out in this direction. Barrat and Chiaruttini[30] calculated the Kapitza length at the solid-liquid interface using both EMD and NEMD methods. They have used a heat flux autocorrelation function at the interface to the calculate Kapitza resistance, which is analogous to the Green-Kubo

Published under license by AIP Publishing

formulas for calculating thermal conductivity. It was pointed out that this method is strictly only true for an infinite system where the heat capacity of the solid and liquid tends to infinity, $C_v \to \infty$. However, the systems used in MD simulations are always finite in nature. For those systems, the running integral of the heat flux autocorrelation function exhibits an exponential decay at long times, from which the Kapitza resistance can be calculated. Rajabpour and Volz[31] proposed an alternative method for calculating the interfacial thermal resistance between crystals using the time integral of the normalized temperature difference autocorrelation function. They defined a characteristic time τ which yields the thermal resistance between two interacting solid bodies having a temperature difference ΔT. Merabia and Termentzidis[32] introduced a method based on the Green-Kubo formulation for calculating the interfacial thermal conductance at the interface between crystals, which is achieved by performing EMD simulations and measuring the decay of thermal energy fluctuations of both crystals. They reported inconsistent results for EMD and NEMD methods. The reason for the discrepancy is because the Green-Kubo method probes the Landauer conductance between two crystals, which assumes an equilibrium between phonons on each crystal forming the interface. Contrarily, NEMD accommodates the out-of-equilibrium thermal conductance at the interface, consistent with the heat flux at the interface, which describes the phonon transport in each crystal. Liang *et al.*[33] have calculated the thermal conductance at solid-gas interfaces with different interfacial interaction potentials with the help of the Green-Kubo method. They found the presence of a layer of adsorbed gas at the solid surface. Therefore, to calculate true interfacial thermal resistance using Green-Kubo formulas, the interface between solid and gas must be defined at a plane outside the adsorbed gas layer. Chalopin *et al.*[34] introduced a new derivation to calculate the interfacial thermal conductance using the EMD method, and the same was used to estimate the thermal conduction mechanism in Si-Ge superlattices. They have compared the results with the Green-Kubo thermal conductivity method and demonstrated that the thermal conductivity of perfect superlattices could be directly inferred from the interfacial conductance within the range of period of their study. This study also emphasized the significance of interfaces in materials with large phonon mean free paths. Kim *et al.*[35] investigated heat transfer between two parallel plates filled by liquid-argon with the help of MD simulations using Lennard-Jones (L-J) potentials. They have characterized the effect of the interfacial thermal resistance for different parameters such as thermal oscillations, surface wettability, wall temperature, frequency, channel height, and thermal gradient. Also, they have developed an empirical model to calculate the Kapitza length, which can be used as the jump coefficient of a Navier boundary condition.

It is clear from the above discussion that Green-Kubo EMD methods provide several advantages in calculating the Kapitza length over NEMD methods in various scenarios. However, all the above-mentioned EMD methods are based on the assumption that the temperature of the system is constant and the temperature fluctuation across the fluid-solid interface is not taken into account for the calculation of the Kapitza length. This motivates us to develop a more direct and potentially accurate EMD method for computing the Kapitza length, which includes both the heat flux *and* the temperature fluctuations at the interface.

This paper introduces such a method for calculating the Kapitza resistance/length at fluid-solid interfaces by considering both the heat flux autocorrelation and heat flux-temperature difference cross-correlation functions. The proposed method is analogous to the study by Hansen *et al.*[36] which developed a new method to predict slip at a fluid-solid interface from analogous correlation functions. The values of the predicted Kapitza length show excellent agreement with both the direct NEMD method and the EMD Green-Kubo method of Barrat and Chiaruttini[30] for different conditions. The theory is derived directly from the definition of the Kapitza resistance and is tested for different simulation conditions by varying parameters such as wetting coefficient, channel width, density, and temperature. The following sections of the paper consist of the derivation of the theory, the methodology adopted for the simulation, discussions about the obtained results, and finally some concluding remarks.

II. THEORY

A. Calculation of the Kapitza resistance

The Kapitza resistance, denoted by the symbol R_k, is defined as

$$R_k = \frac{\Delta T}{J_q}, \tag{3}$$

where $\Delta T = T_f - T_w$ is the difference between the temperature of the layer of fluid immediately adjacent to the wall, T_f, and the temperature of the wall, T_w, and J_q is the component of the heat flux vector normal to the wall.

In what follows, we consider a liquid-solid system at equilibrium. For the case of time dependence of the Kapitza kernel, we can write the instantaneous governing constitutive equation [Eq. (3)] as

$$\Delta T(t) = \int_0^t R_k(t-t')J_q(t')dt' + T_R(t), \tag{4}$$

where $T_R(t)$ is a random thermal noise term with zero mean and which is uncorrelated with the heat flux, namely,

$$\langle T_R(t)\rangle = 0 \quad \text{and} \quad \langle J_q(0)T_R(t)\rangle = 0. \tag{5}$$

Here, we have assumed that we can ignore nonlocal effects induced by fluid structural inhomogeneity as was assumed by Hansen *et al.*[36] Multiplying Eq. (4) by $J_q(t=0)$ and taking the ensemble average we get

$$\begin{aligned}\langle J_q(0)\Delta T(t)\rangle &= \left\langle J_q(0)\int_0^t R_k(t-t')J_q(t')dt'\right\rangle \\ &= \left\langle \int_0^t R_k(t-t')J_q(0)J_q(t')dt'\right\rangle \\ &= \int_0^t R_k(t-t')\langle J_q(0)J_q(t')\rangle dt'. \end{aligned} \tag{6}$$

If we define the time-correlation functions as $C_{TJ_q}(t) \equiv \langle J_q(0)\Delta T(t)\rangle$ and $C_{J_qJ_q}(t) \equiv \langle J_q(0)J_q(t)\rangle$, Eq. (6) can be expressed as

Published under license by AIP Publishing

$$C_{TJ_q}(t) = \int_0^t R_k(t-t')C_{J_qJ_q}(t')dt'. \tag{7}$$

We define the Laplace transform of some arbitrary function $f(t)$ as

$$L(f(t)) \equiv \int_0^\infty f(t)e^{-st}dt \equiv \tilde{f}(s). \tag{8}$$

Note that as a consequence, we have

$$\tilde{f}(s=0) = \int_0^\infty f(t)dt, \tag{9}$$

which is the time-independent steady-state value of f. Thus, taking the Laplace transform of Eq. (7) gives

$$\tilde{C}_{TJ_q}(s) = \tilde{R}_k(s)\tilde{C}_{J_qJ_q}(s). \tag{10}$$

Now, the Kapitza resistance can be evaluated directly via Eq. (10), i.e.,

$$\tilde{R}_k(s) = \frac{\tilde{C}_{TJ_q}(s)}{\tilde{C}_{J_qJ_q}(s)}, \tag{11}$$

from which $R_k \equiv \tilde{R}_k(s=0)$ can be extracted. This procedure, while reasonable, may in fact be an inefficient and statistically noisy way to extract R_k. A more efficient method may be to extract $\tilde{R}_k(s)$ by fitting the right-hand side of Eq. (10) to the left-hand side of that same equation and then extracting the $s = 0$ value directly. This would generate a statistically more accurate value since we are using all the available data not just the $s = 0$ value.

Furthermore, as identified by Hansen *et al.*,[36] if we assume that R_k has a Maxwellian distribution in time, we can express this time-dependence as[10]

$$R_k(t) = \sum_{i=1}^n k_i e^{-\mu_i t}. \tag{12}$$

Taking the Laplace transform of this gives

$$\tilde{R}_k(s) = \sum_{i=1}^n \frac{k_i}{s+\mu_i}. \tag{13}$$

Substituting Eq. (13) into Eq. (10) gives

$$\tilde{C}_{TJ_q}(s) = \sum_{i=1}^n \frac{k_i}{s+\mu_i}\tilde{C}_{J_qJ_q}(s). \tag{14}$$

Therefore, for steady-state conditions ($s = 0$), we have

$$R_k \equiv \tilde{R}_k(0) = \sum_{i=1}^n \frac{k_i}{\mu_i}. \tag{15}$$

Using EMD simulations, we can compute $C_{TJ_q}(t)$ and $C_{J_qJ_q}(t)$ and the corresponding Laplace transforms. From these data, we can fit the right-hand side of Eq. (14) to the $\tilde{C}_{TJ_q}(s)$ and $\tilde{C}_{J_qJ_q}(s)$ data using k_i and μ_i as fitting parameters.

B. Calculation of the heat flux

The heat flux across the fluid-solid interface is one of the most important parameters in the calculation of the Kapitza resistance. The expression of heat flux for inhomogeneous fluids can be split into kinetic and potential terms. For a system with a temperature gradient in the z-direction (such as the case in our geometry; see Fig. 2), the instantaneous heat flux calculated at a plane located at z with surface area A, $J_{qz}(z, t)$, can be computed from the method of planes technique of Todd *et al.*,[37,38]

$$J_{qz}(z,t) = J^K_{qz}(z,t) + J^\phi_{qz}(z,t), \tag{16}$$

where the kinetic term is given by

$$J^K_{qz}(z,t) = \frac{1}{A}\sum_i (v_{zi} - v_z(z_i))u_i\delta(z-z_i) \tag{17}$$

and the potential term is given by

$$J^\phi_{qz}(z,t) = \frac{1}{4A}\sum_{i,j}[\mathbf{v}_i - \mathbf{v}(z)]\cdot\mathbf{F}^\phi_{ij}[sgn(z_i - z) - sgn(z_j - z)]. \tag{18}$$

In Eq. (17), u_i is the total internal energy of particle i, defined such that the streaming kinetic energy is now subtracted out of the energy density, i.e.,

$$u_i = \frac{1}{2}m\mathbf{c}_i^2 + \frac{1}{2}\sum_j \phi_{ij}, \tag{19}$$

where $\mathbf{c}_i$ is the "peculiar" or thermal velocity of particle i, namely, $\mathbf{c}_i \equiv \mathbf{v}_i - \mathbf{v}(z)$, $\mathbf{v}_i$ is its laboratory velocity, and $\mathbf{v}(z)$ is the fluid streaming velocity at z. For systems under no flow (such as in this current study), $\mathbf{v}(z) = 0$ and $\mathbf{c}_i = \mathbf{v}_i$. ϕ_{ij} and $\mathbf{F}^\phi_{ij}$ are the potential energy and interatomic force between particles i and j, respectively.

The contribution of the kinetic part is, in general, not negligible for a dense fluid system.[38] However, it is found from simulations that, at planes adjacent to the fluid-solid interface, there is a small region in which no or negligible particles cross them. In other words, there is a density depletion region created adjacent to the interface which restricts the movement of fluid particles across this region. This plane is taken as the interface between the solid and fluid. Since negligible number of particles cross this plane, the kinetic term is very small at the interface and can be safely ignored. Therefore, the heat flux at the interface can be considered to be almost solely due to the contribution from the potential term, so only Eq. (18) is used in its computation. Equations (16)–(18) are valid for both the EMD and NEMD simulations we performed in this study.

III. METHODOLOGY

Equilibrium and nonequilibrium molecular dynamics simulations were carried out to investigate the Kapitza resistance at the fluid-solid interface. All the simulations were performed by using the LAMMPS[39] package. The interactions between particles are of the Lennard-Jones form, and the quantities are given in standard dimensionless molecular dynamics units. The L-J parameters, σ and ε, are set to unity as reference values. The L-J potential is given by

$$\phi_{ij}(r) = 4\varepsilon\left[\left(\frac{\sigma}{r}\right)^{12} - C_{ij}\left(\frac{\sigma}{r}\right)^6\right]. \tag{20}$$

Published under license by AIP Publishing

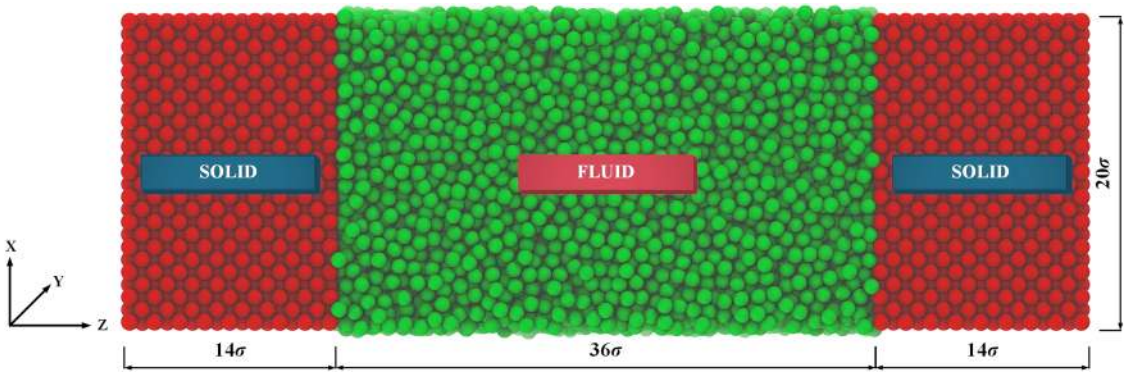

FIG. 1. Schematic depiction of the simulation box consists of fluid confined between two solid slabs.

To model different wetting properties at the interface, the strength of the attractive term was controlled by a wetting coefficient C_{ij} (which can also be achieved by introducing different combinations of values to σ and ε pairs). The fluid-fluid interaction C_{11} was taken as 1.2, solid-solid interaction C_{22} was taken as 1.0, and the fluid-solid interaction C_{12} was varied between 1.0 and 0.5. By tuning the fluid-solid interaction strength C_{12} from 1.0 to 0.5, we can attain a contact angle that varies from $\theta \approx 90^\circ$ to $\theta \approx 140^\circ$, which corresponds to the range of fluid-solid surface properties from wetting to nonwetting situations.[40] The effect of fluid channel width was studied by varying the channel width, l, from 6 to 42 σ. To study the effect of fluid density, ρ, on the Kapitza length, different simulations were performed by changing ρ from 0.7 to 1.3. Finally, simulations at various reference temperatures ranging from 0.9 to 1.2 were also performed. The cutoff distance for the L-J potential was taken as 2.5 σ.

The simulation domain consists of a fluid block confined between two parallel solid slabs, as shown in Fig. 1. The dimensions for that particular system are $L_x = 20$, $L_y = 20$, and $L_z = 64$, in which the fluid block thickness is 36 and each solid slab has a thickness of 14. Periodic boundary conditions were given in x and y directions, and confinement was in the z-direction. The solid atoms were initially arranged in an fcc structure with (100) orientation with a density of 0.9. The solid atoms were tethered around their initial lattice positions $\mathbf{r}_{eq}$ using a weak harmonic spring potential, $\phi_s = \frac{1}{2}k_s(\mathbf{r}_i - \mathbf{r}_{eq})^2$, where the spring constant k_s was taken as 150.[36] The fluid density was kept at 0.88, and all the simulations were carried out at a reference temperature $T = 1$, ensuring we were in the liquid phase. For EMD simulations, the wall temperature was maintained at the reference temperature by using a Nosé-Hoover thermostat.[41,42] The equations of motion for solid and fluid atoms were integrated using a leap-frog integration scheme[43] with a time step $\Delta t = 0.001$. All the results were averaged over five independent simulations with different initial configurations.

For EMD simulations, the instantaneous heat flux at the fluid-solid interface was calculated using Eq. (16). As previously noted, the contribution of the kinetic term of heat flux is negligible compared to the potential term at interfaces. In addition, the instantaneous temperature difference ΔT between the wall and the adjacent fluid slab was also calculated. The calculation of the Kapitza length using the newly introduced method is described in Sec. II.

NEMD simulations were carried out to verify the proposed EMD method. In this case, a temperature gradient was created along the z-direction to compute the Kapitza resistance. Two different temperatures (0.9 and 1.1) were maintained at the two outermost layers of the two solid walls with the implementation of a Nosé-Hoover thermostat. The Kapitza resistance R_k is computed directly from Eq. (3), where ΔT is the temperature difference at the interface and J_q is the average heat flux across the interface. The temperature difference is calculated from the temperature profile along the z-direction, and J_q is calculated from the energy added/subtracted from the thermostated region per unit time across the unit interface area. Table I shows the average ΔT as a function of wetting coefficient C_{12}. NEMD simulations were carried out over long enough time durations to obtain a steady-state heat flux and a linear temperature profile. The Kapitza length was calculated by Eq. (2), and the thermal conductivity of the solid and fluid was calculated from the temperature profile obtained from NEMD simulations using Fourier's law. The thermal conductivity of the fluid was used for the calculation of the Kapitza length in all the cases. In addition to this, the EMD method for calculating the Kapitza length derived from the Green-Kubo method of Barrat and Chiaruttini[30] was also used for comparing our proposed new method. This method is itself

TABLE I. The average temperature difference, ΔT, quoted to 6 decimal place accuracy, at the interface for different wetting coefficients obtained from NEMD simulations.

Wetting coefficient (C_{12})	Temperature drop at the interface (ΔT)
0.5	0.030 088
0.6	0.022 592
0.7	0.016 677
0.8	0.014 455
0.9	0.010 658
1.0	0.005 373

Published under license by AIP Publishing

based on a Langevin dynamics model inspired by Puech *et al.*[44] and is expressed here as

$$\frac{1}{R_k} = \frac{A}{k_B T^2} \int_0^\infty dt \langle J_{qz}(t) J_{qz}(0) \rangle, \tag{21}$$

where k_B is the Boltzmann constant (set here to 1). $J_{qz}(t)$ is the heat flux across the interface of surface area A and is computed from the work per unit time performed by the solid atoms on liquid atoms,[30]

$$J_{qz}(t) = \frac{1}{A} \sum_{i \in liquid} \sum_{j \in solid} \mathbf{F}_{ij}^{\phi} \cdot \mathbf{v}_i. \tag{22}$$

This is effectively the same as the heat flux expression given in Eq. (18), which is what is used in both EMD methods to allow direct comparison between them.

Finally, we make the observation that the heat flux computed by Barrat and Chiaruttini[30] [Eq. (22)] excludes the kinetic contribution. As we have pointed out in the above discussion, if the interface region is such that the kinetic contribution is minimal, then it can be neglected, but it should formally be included in the total heat flux expression.

IV. RESULTS AND DISCUSSION

The temperature profile obtained from NEMD simulations for a wall-fluid wetting coefficient, $C_{12} = 0.5$, is shown in Fig. 2. The maximum standard error in the temperature profile across the entire fluid channel is found to be ~0.35%. The temperature profile in the solid and fluid region varies linearly with the position, which satisfies the predictions of Fourier's law. The thermal conductivity of the fluid and solid is calculated from the slope of the linear regime of the temperature profile. The values of thermal conductivity obtained are 9.6 ± 0.7 and 8.4 ± 0.5 for bulk solid and fluid, respectively.

Figure 3 shows the normalized heat flux autocorrelation function, $C_{J_qJ_q}$, for different wetting coefficients and for short times. The correlation function decays to zero at longer times as expected. The normalized correlation function between heat flux and temperature difference C_{J_qT} for different wetting coefficients is shown in Fig. 4. It is observed that the heat flux and temperature difference

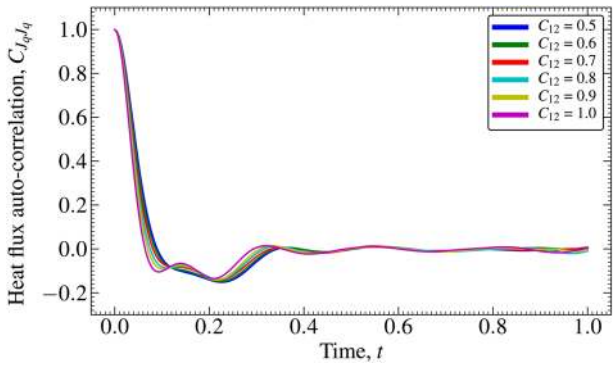

FIG. 3. Normalized heat flux autocorrelation function for different wetting coefficients.

are initially anticorrelated, which is because heat flux flows in the direction opposite to the temperature drop across the interface. The correlation function then decays to zero within 0.8–1.0 time units, which is about two times higher than the correlation window of the heat flux autocorrelation function. Both the correlation functions $C_{J_qJ_q}$ and C_{J_qT} are calculated during the EMD simulations by using the instantaneous heat flux and temperature difference at the interface, which is measured throughout the simulation period. The Green-Kubo based EMD method only uses the heat flux autocorrelation function, for which the correlation window is about two times less than heat flux-temperature difference correlation function. Due to this smaller correlation window, the simulation time required to get similar statistics is smaller compared to our new EMD method. Even though the present method takes more simulation time, it also incorporates the temperature fluctuation at the interface, thus using more of the information available in the simulation. Our method also obviates the need to ensure that the time correlation functions fully decay to zero as is needed in any Green-Kubo method. Furthermore, by limiting the correlation functions to an interface region of width Δ, we can be sure that the Kapitza resistance we compute is a local interfacial and not a bulk fluid property.

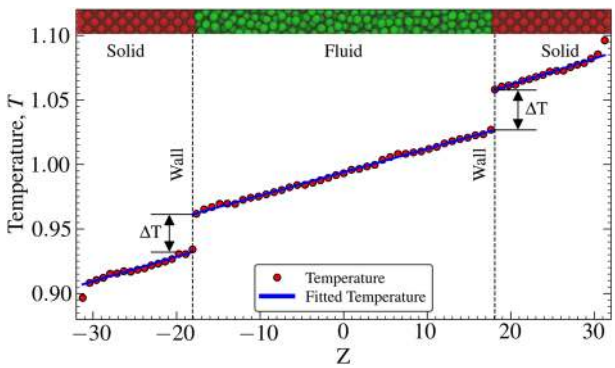

FIG. 2. Temperature profile obtained from NEMD simulation for a wetting coefficient $C_{12} = 0.5$.

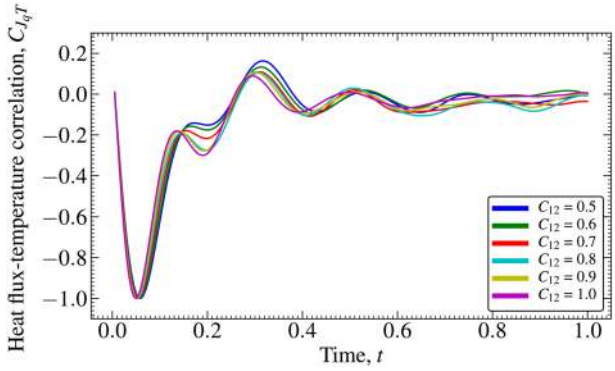

FIG. 4. Normalized heat flux-temperature cross-correlation function for different wetting coefficients.

Published under license by AIP Publishing

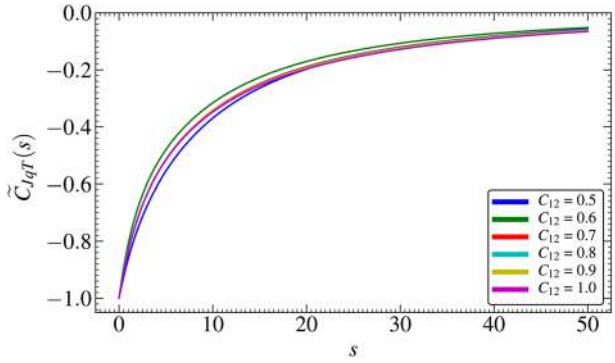

FIG. 5. Normalized Laplace transform of the heat flux-temperature cross-correlation function for different wetting coefficients.

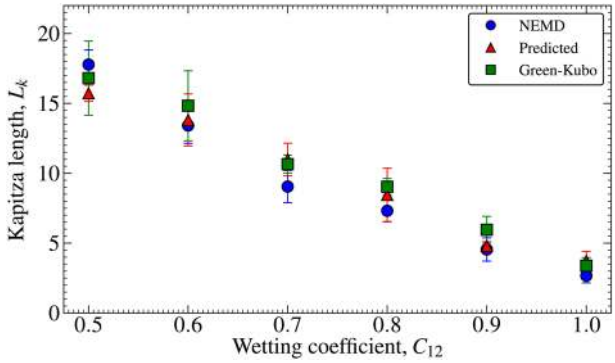

FIG. 7. The variation of the predicted Kapitza length as a function of the wetting coefficient. The results are compared with NEMD simulations and the Green-Kubo method of Barrat and Chiaruttini.[30]

The Laplace transform of the correlation function data was calculated using a simple trapezoidal integration method. The normalized Laplace transform of the heat flux-temperature difference cross-correlation function, $\tilde{C}_{TJ_q}(s)$, for different wetting coefficients is shown in Fig. 5. The $\tilde{C}_{TJ_q}(s)$ and $\tilde{C}_{J_qJ_q}(s)$ data are fitted with Eq. (14), and the fitting parameters μ_i and k_i are used to calculate the Kapitza resistance for steady-state conditions ($s = 0$) from Eq. (15). It is found that a Maxwellian one term ($n = 1$) memory function is adequate to describe the relation between $C_{J_qJ_q}$ and C_{TJ_q}. This applies to all the cases in this study. The dependency of the fluid slab thickness on the Kapitza length is shown in Fig. 6. The selection of the fluid slab thickness is significant in calculating the Kapitza length. If the thickness is too small, there will not be enough fluid particles to compute the properties at the slab. If the thickness is too large, then the computed properties will be bulk fluid properties. To find the optimum slab thickness, the Kapitza length for different slab thicknesses, Δ, ranging from 0.2 to 5 was calculated. From Fig. 6, it can be seen that for small slab thickness, the values of the Kapitza length are very large and statistically noisy. As the slab thickness increases, the uncertainty reduces, and the values of the Kapitza length remain stable at about Δ = 2.0 for all types of interfaces. Therefore, the slab thickness is taken as 2.0 for further calculations in this study.

Figure 7 shows the comparison of our predicted Kapitza length with both the direct NEMD method and the Green-Kubo method by Barrat and Chiaruttini[30] for different wetting coefficients. The wetting coefficient varied between 0.5 and 1.0 imitating a hydrophobic to a hydrophilic interface. The plot shows that the predicted value of the Kapitza length is in excellent agreement with the results of both NEMD and Green-Kubo methods for all the wetting coefficients and serves as a validation for our method. It is found that the Kapitza length decreases with an increase in the wetting coefficient, in agreement with the results of Tascini *et al.*[24] The higher the wetting coefficient, the higher the wettability of fluid particles on the wall. When a higher number of fluid particles are immediately adjacent to the wall, the thermal resistance across the interface will reduce. Thus, the temperature drop at the interface will reduce and heat flux across the interface will increase, causing a reduction in the Kapitza resistance. The variation of the Kapitza length as a function of fluid channel width, l, for $C_{12} = 0.5$ is plotted in Fig. 8. Different channel widths ranging from 6 to 42 were used to model the system. From the plot, we can see that the uncertainty in the Kapitza

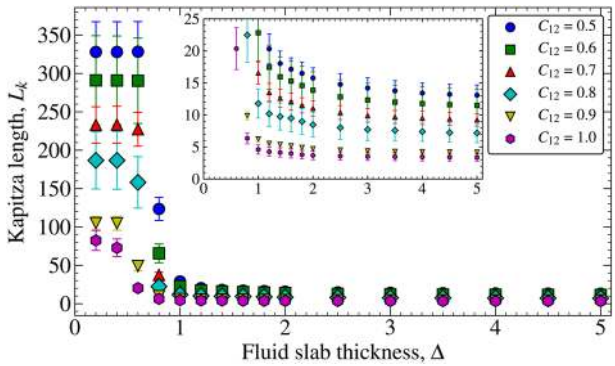

FIG. 6. Kapitza length as a function of fluid slab thickness for different wetting coefficients. The inset shows the Kapitza length to a maximum of 25 to magnify the scale.

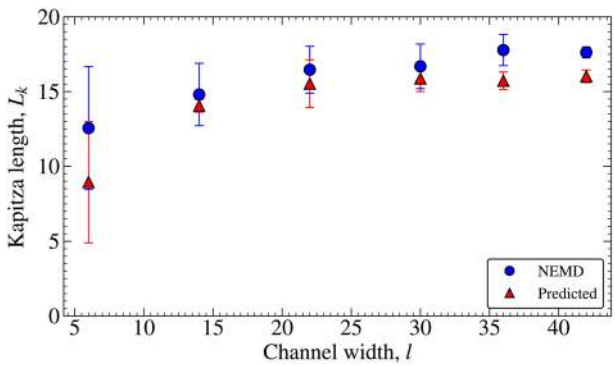

FIG. 8. The variation of the predicted Kapitza length as a function of the fluid channel width. The results are compared with NEMD simulations.

Published under license by AIP Publishing

length is much higher for smaller channel width. For larger channel widths, the uncertainty reduces and the values remain constant with a further increase in channel width. Liang and Tsai[45] have reported a similar result in which they found a rapid increase in the Kapitza resistance with an increase in fluid film thickness. The Kapitza resistance is one order of magnitude smaller if the fluid thickness is one molecular layer and increases rapidly with the addition of fluid layers. The size effects in the simulation results are visible in this plot. The selection of system size is very crucial in MD simulations for calculating the Kapitza resistance. A channel width of $l = 36$ is used throughout this study, which was the width where convergence of the Kapitza length was found. The predicted results are in excellent agreement with direct NEMD simulation results.

We also note here that our formalism, along with those that use a Green-Kubo formulation, ignores nonlocal transport effects. Such effects may become important at extreme confinement lengths as has been shown in the case of momentum transport (see the book by Todd and Daivis[37] and references therein as well as the recent work by Camargo and colleagues[46,47]). Such an investigation is beyond the scope of this current study, in which our local model is seen to work well for the nanoscale confinement dimensions probed here. Figure 9 shows the variation of the Kapitza length as a function of fluid density for $C_{12} = 0.5$. The density varied between 0.7 and 1.3, and it is found that the Kapitza length reduces with an increase in the density. For the higher density systems and, in particular, for the two highest density systems studied (where now the "fluid" is actually in the solid phase), the number of particles adjacent to the interface will be higher, which helps to improve the heat transfer between these interface layers and causes a reduction in the Kapitza resistance. From the above, we can conclude that the Kapitza length will reduce if we increase the density of the fluid while keeping all other variables unaltered. The predicted results are also in good agreement with our NEMD simulations.

Several studies reported the dependency of temperature on the Kapitza resistance.[2,48,49] It is observed that the Kapitza resistance tends to reduce with an increase in temperature of the system. However, these observations are limited to a particular range of temperatures, type of interfaces, and material type. Also, the thermal conductivity of the material is a function of temperature, which is a variable in calculating the Kapitza length [Eq. (2)]. Thus, it is not possible to generalize the temperature dependency of the Kapitza length since it depends on other factors also. The effect of temperature of the system on the Kapitza length for $C_{12} = 0.5$ is shown in Fig. 10. The reference temperature of the system changed from 0.9 to 1.2, and we find that the Kapitza length tends to reduce with an increase in temperature for this particular interface. However, this trend can vary depending upon other factors of the system, such as type of interfaces, type of materials, and range of temperatures. The predicted results are again compared with NEMD simulations and show good agreement.

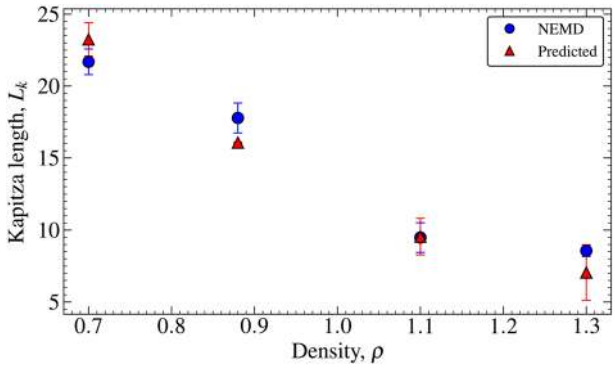

FIG. 9. The variation of the predicted Kapitza length as a function of density. The results are compared with NEMD simulations.

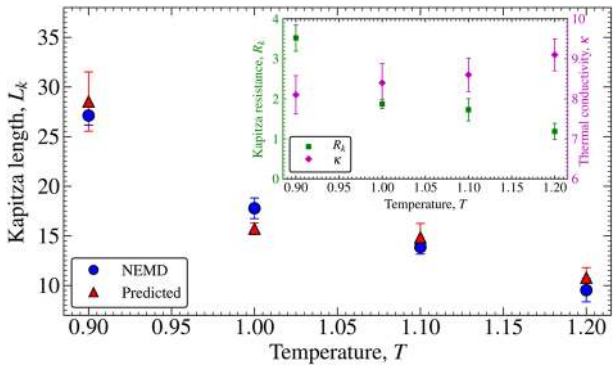

FIG. 10. The variation of the predicted Kapitza length as a function of temperature. The results are compared with NEMD simulations. The inset shows the variation of the Kapitza resistance and fluid thermal conductivity as a function of temperature.

V. CONCLUSION

The calculation of the interfacial thermal resistance plays a crucial role in nanoscale heat transfer problems and systems. The present work introduces a new method to compute the Kapitza length at a fluid-solid interface accurately using EMD simulations. A theoretical framework is developed, and the same is validated using classical molecular dynamics simulations. The simulation domain consists of a Lennard-Jones system with fluid confined between two solid slabs. Different kinds of interfaces are tested by modifying the fluid-solid energy of interaction, which is achieved by varying the wetting coefficient at the interface. In addition to that, simulations at different conditions such as channel width, density, and temperature were also carried out. The proposed method is validated by using NEMD and equilibrium Green-Kubo methods. The Kapitza resistance and thermal conductivities of the solid and fluid are directly calculated from NEMD simulations by providing a temperature gradient across the system. It is observed that the Kapitza length reduces with increasing the wetting coefficient, and the values are in excellent agreement with the NEMD and Green-Kubo results for corresponding wetting coefficients. Thus, our proposed method could be used in any interface ranging from hydrophobic to hydrophilic as well as solid-solid interfaces (as shown in Fig. 9). It may be particularly useful for complex fluids where the equilibrium heat flux time autocorrelation function decays slowly, making Green-Kubo calculations difficult due to nonconvergence of the time integral.

Published under license by AIP Publishing

These results provide relevant insight into the Kapitza length in fluid-solid interfaces. Calculating the Kapitza length from EMD simulations has significant advantages over NEMD methods. NEMD simulations require a considerable temperature gradient across the interface to collect sufficient statistics. Due to this higher temperature gradient, there is a chance of obtaining a nonlinear response, which deviates from the response that is of experimental interest. Since the proposed EMD method evaluates the linear response of the system, it does not suffer from this limitation. Moreover, for higher values of wetting coefficient (hydrophilic surface), the temperature difference at the interface is extremely low, such that the direct calculation of the Kapitza resistance from Eq. (1) becomes difficult. The Kapitza resistance is highly sensitive to even a small change in the temperature difference at the interface for the NEMD approach. Thus, our proposed EMD method overcomes these challenges and provides an efficient and accurate way to calculate the Kapitza resistance and length at fluid-solid interfaces. This in turn can be used to predict the temperature profile of the system precisely without the need to do NEMD simulations.

In future work, we will demonstrate how our equilibrium MD method can be used to predict the Kapitza length for confined fluids under flow conditions, particularly for superhydrophobic systems such as water in graphene channels or carbon nanotubes, where frictional forces are minimal and so too energy dissipation. For such systems, both velocity and temperature profiles are almost flat, making NEMD measurements of slip and Kapitza lengths very difficult (see, for example, the work of Kannam *et al.*[16,50]).

Note added in proof. The stable convergence of the Kapitza length (or Kapitza resistance) as a function of fluid slab thickness as shown in Fig. 6 suggests the slab thickness could be extended to cover the entire fluid channel volume, rather than just a narrow interfacial volume. We are conducting further simulations to verify this and will publish our findings in a subsequent paper.

ACKNOWLEDGMENTS

The authors acknowledge the P. G. Senapathy Center for Computing Resource at IIT Madras and the Swinburne University Supercomputer Centre for providing computational resources for this work.

REFERENCES

[1] G. Karniadakis, A. Beskok, and N. Aluru, *Microflows and Nanoflows: Fundamentals and Simulation* (Springer Science & Business Media, 2006), Vol. 29.
[2] D. G. Cahill, W. K. Ford, K. E. Goodson, G. D. Mahan, A. Majumdar, H. J. Maris, R. Merlin, and S. R. Phillpot, "Nanoscale thermal transport," J. Appl. Phys. **93**, 793–818 (2003).
[3] E. Pop, "Energy dissipation and transport in nanoscale devices," Nano Res. **3**, 147–169 (2010).
[4] P. Kapitza, "The study of heat transfer in helium II," J. Phys. USSR **4**, 181 (1941).
[5] I. M. Khalatnikov, *An Introduction to the Theory of Superfluidity* (CRC Press, 2018).
[6] L. Bocquet and J.-L. Barrat, "Hydrodynamic boundary conditions, correlation functions, and Kubo relations for confined fluids," Phys. Rev. E **49**, 3079 (1994).
[7] S. K. Kannam, B. D. Todd, J. S. Hansen, and P. J. Daivis, "Slip flow in graphene nanochannels," J. Chem. Phys. **135**, 144701 (2011).
[8] J.-P. Hansen and I. R. McDonald, *Theory of Simple Liquids: With Applications to Soft Matter* (Academic Press, 2013).
[9] W. G. Hoover, "Nonequilibrium molecular dynamics," Annu. Rev. Phys. Chem. **34**, 103–127 (1983).
[10] D. J. Evans and G. Morriss, *Statistical Mechanics of Nonequilibrium Liquids* (Cambridge University Press, 2008).
[11] Z. Liang and M. Hu, "Tutorial: Determination of thermal boundary resistance by molecular dynamics simulations," J. Appl. Phys. **123**, 191101 (2018).
[12] M. R. Hasan, T. Q. Vo, and B. Kim, "Manipulating thermal resistance at the solid–fluid interface through monolayer deposition," RSC Adv. **9**, 4948–4956 (2019).
[13] Y.-J. Wu, L. Fang, and Y. Xu, "Predicting interfacial thermal resistance by machine learning," npj Comput. Mater. **5**, 56 (2019).
[14] S. Chen, M. Yang, B. Liu, M. Xu, T. Zhang, B. Zhuang, D. Ding, X. Huai, and H. Zhang, "Enhanced thermal conductance at the graphene–water interface based on functionalized alkane chains," RSC Adv. **9**, 4563–4570 (2019).
[15] Y. Ma, Z. Zhang, J. Chen, K. Sääskilahti, S. Volz, and J. Chen, "Ordered water layer induced by interfacial charge decoration leads to an ultra-low Kapitza resistance between graphene and water," Carbon **135**, 263–269 (2018).
[16] S. K. Kannam, B. D. Todd, J. S. Hansen, and P. J. Daivis, "Slip length of water on graphene: Limitations of non-equilibrium molecular dynamics simulations," J. Chem. Phys. **136**, 024705 (2012).
[17] E. Landry and A. McGaughey, "Thermal boundary resistance predictions from molecular dynamics simulations and theoretical calculations," Phys. Rev. B **80**, 165304 (2009).
[18] R. E. Jones, J. Duda, X. Zhou, C. Kimmer, and P. Hopkins, "Investigation of size and electronic effects on Kapitza conductance with non-equilibrium molecular dynamics," Appl. Phys. Lett. **102**, 183119 (2013).
[19] T. Watanabe, B. Ni, S. R. Phillpot, P. K. Schelling, and P. Keblinski, "Thermal conductance across grain boundaries in diamond from molecular dynamics simulation," J. Appl. Phys. **102**, 063503 (2007).
[20] Z. Liang, K. Sasikumar, and P. Keblinski, "Thermal transport across a substrate–thin-film interface: Effects of film thickness and surface roughness," Phys. Rev. Lett. **113**, 065901 (2014).
[21] Z. Liang and P. Keblinski, "Finite-size effects on molecular dynamics interfacial thermal-resistance predictions," Phys. Rev. B **90**, 075411 (2014).
[22] S. Merabia, S. Shenogin, L. Joly, P. Keblinski, and J.-L. Barrat, "Heat transfer from nanoparticles: A corresponding state analysis," Proc. Natl. Acad. Sci. U. S. A. **106**, 15113–15118 (2009).
[23] A. Lervik, F. Bresme, and S. Kjelstrup, "Heat transfer in soft nanoscale interfaces: The influence of interface curvature," Soft Matter **5**, 2407–2414 (2009).
[24] A. S. Tascini, J. Armstrong, E. Chiavazzo, M. Fasano, P. Asinari, and F. Bresme, "Thermal transport across nanoparticle fluid interfaces: The interplay of interfacial curvature and nanoparticle fluid interactions," Phys. Chem. Chem. Phys. **19**, 3244 (2017).
[25] J. Muscatello, E. Chacón, P. Tarazona, and F. Bresme, "Deconstructing temperature gradients across fluid interfaces: The structural origin of the thermal resistance of liquid-vapor interfaces," Phys. Rev. Lett. **119**, 045901 (2017).
[26] H. Hu and Y. Sun, "Effect of nanopatterns on Kapitza resistance at a water-gold interface during boiling: A molecular dynamics study," J. Appl. Phys. **112**, 053508 (2012).
[27] A. Pham, M. Barisik, and B. Kim, "Pressure dependence of Kapitza resistance at gold/water and silicon/water interfaces," J. Chem. Phys. **139**, 244702 (2013).
[28] B. Ramos-Alvarado, S. Kumar, and G. Peterson, "Solid–liquid thermal transport and its relationship with wettability and the interfacial liquid structure," J. Phys. Chem. Lett. **7**, 3497–3501 (2016).
[29] H. Han, S. Merabia, and F. Müller-Plathe, "Thermal transport at a solid–nanofluid interface: From increase of thermal resistance towards a shift of rapid boiling," Nanoscale **9**, 8314–8320 (2017).
[30] J.-L. Barrat and F. Chiaruttini, "Kapitza resistance at the liquid—Solid interface," Mol. Phys. **101**, 1605–1610 (2003).

Published under license by AIP Publishing

[31] A. Rajabpour and S. Volz, "Thermal boundary resistance from mode energy relaxation times: Case study of argon-like crystals by molecular dynamics," J. Appl. Phys. **108**, 094324 (2010).
[32] S. Merabia and K. Termentzidis, "Thermal conductance at the interface between crystals using equilibrium and nonequilibrium molecular dynamics," Phys. Rev. B **86**, 094303 (2012).
[33] Z. Liang, W. Evans, and P. Keblinski, "Equilibrium and nonequilibrium molecular dynamics simulations of thermal conductance at solid-gas interfaces," Phys. Rev. E **87**, 022119 (2013).
[34] Y. Chalopin, K. Esfarjani, A. Henry, S. Volz, and G. Chen, "Thermal interface conductance in Si/Ge superlattices by equilibrium molecular dynamics," Phys. Rev. B **85**, 195302 (2012).
[35] B. H. Kim, A. Beskok, and T. Cagin, "Molecular dynamics simulations of thermal resistance at the liquid-solid interface," J. Chem. Phys. **129**, 174701 (2008).
[36] J. S. Hansen, B. D. Todd, and P. J. Daivis, "Prediction of fluid velocity slip at solid surfaces," Phys. Rev. E **84**, 016313 (2011).
[37] B. D. Todd and P. J. Daivis, *Nonequilibrium Molecular Dynamics: Theory, Algorithms and Applications* (Cambridge University Press, 2017).
[38] B. D. Todd, P. J. Daivis, and D. J. Evans, "Heat flux vector in highly inhomogeneous nonequilibrium fluids," Phys. Rev. E **51**, 4362 (1995).
[39] S. Plimpton, "Fast parallel algorithms for short-range molecular dynamics," J. Comput. Phys. **117**, 1–19 (1995).
[40] J.-L. Barrat and L. Bocquet, "Large slip effect at a nonwetting fluid-solid interface," Phys. Rev. Lett. **82**, 4671 (1999).
[41] S. Nosé, "A molecular dynamics method for simulations in the canonical ensemble," Mol. Phys. **52**, 255–268 (1984).
[42] W. G. Hoover, "Canonical dynamics: Equilibrium phase-space distributions," Phys. Rev. A **31**, 1695 (1985).
[43] D. Frenkel and B. Smit, *Understanding Molecular Simulation: From Algorithms to Applications* (Elsevier, 2001), Vol. 1.
[44] R. Puech, G. Bonfait, and B. Castaing, "Mobility of the ^{3}He solid-liquid interface: Experiment and theory," J. Low Temp. Phys. **62**, 315 (1986).
[45] Z. Liang and H.-L. Tsai, "Effect of molecular film thickness on thermal conduction across solid-film interfaces," Phys. Rev. E **83**, 061603 (2011).
[46] D. Camargo, J. de la Torre, D. Duque-Zumajo, P. Espanol, R. Delgado-Buscalioni, and F. Chejne, "Nanoscale hydrodynamics near solids," J. Chem. Phys. **148**, 064107 (2018).
[47] D. Camargo, J. de la Torre, R. Delgado-Buscalioni, F. Chejne, and P. Espanol, "Boundary conditions derived from a microscopic theory of hydrodynamics near solids," J. Chem. Phys. **150**, 144104 (2019).
[48] H.-S. Yang, G.-R. Bai, L. Thompson, and J. Eastman, "Interfacial thermal resistance in nanocrystalline yttria-stabilized zirconia," Acta Mater. **50**, 2309–2317 (2002).
[49] A. Chernatynskiy, X.-M. Bai, and J. Gan, "Systematic investigation of the misorientation-and temperature-dependent Kapitza resistance in CeO_2," Int. J. Heat Mass Transfer **99**, 461–469 (2016).
[50] S. K. Kannam, B. D. Todd, J. S. Hansen, and P. J. Daivis, "How fast does water flow in carbon nanotubes?," J. Chem. Phys. **138**, 094701 (2013).

Published under license by AIP Publishing